Iranian Journal of Numerical Analysis and Optimization
Vol. 13, No. 2, 2023, pp 317–335
https://doi.org/10.22067/ijnao.2022.79205.1190
https://ijnao.um.ac.ir/

Research Article

Two-layer shallow water formula with slope and uneven bottom solved by finite volume method

U. Habibah*, I.R Lina, and W.M Kusumawinahyu

Abstract

This paper proposes a numerical approach to solve a two-layer shallow water formula with a slope and uneven bottom. The finite volume method (FVM) is applied to solve the shallow water model because the method is suitable for computational fluid dynamics problems. Rather than pointwise approximations at grid points, the FVM breaks the domain into grid cells and approximates the total integral over grid cells. The shallow water model is examined in two cases, the shallow water model in the steady state and the unsteady state. The quadratic upstream interpolation for convective kinetics (QUICK) is chosen to get the discretization of the space domain since it is a third-order scheme, which provides good accuracy, and this scheme proves its numerical stability. The advantage of the QUICK method is that the main coefficients are positive and satisfy the requirements for conservativeness, boundedness, and transportation. An explicit scheme is used to get the discretization of the time domain. Finally, the numerical solution of the steady state model shows that the flow remains unchanged. An unsteady-state numerical solution produces instability (wavy at the bottom layer). Moreover, the larger slope results in higher velocity and higher depth at the second layer.

*Corresponding author

Received 16 October 2022; revised 3 December 2022; accepted 13 December 2022

Ummu Habibah
Department of Mathematics, Faculty of Mathematics and Natural Sciences, University of Brawijaya, Malang, Indonesia. e-mail: ummu_habibah@ub.ac.id

Ismi Rizqa Lina
Department of Data Science, University of Insan Cita Indonesia, Jakarta, Indonesia. e-mail: ismi@uici.ac.id

Wuryansari Muharini Kusumawinahyu
Department of Mathematics, Faculty of Mathematics and Natural Sciences, University of Brawijaya, Malang, Indonesia. e-mail: wmuharini@ub.ac.id

AMS subject classifications (2020): Primary 76-10, 65M08.

Keywords: Two-layer shallow water; Finite volume method; QUICK scheme; Explicit scheme.

1 Introduction

A flow with constant density where the horizontal scale is much bigger than the vertical scale is called shallow water. Shallow water is a thin layer of fluid of constant density in hydrostatic equilibrium, surrounded by a solid surface below and a free surface above, and is likely in contact with another low-inertia fluid. The simplest and most useful models in geophysical fluid dynamics are single-layer models because they can explain the rotational effect with a simple structure without considering the effects of complex stratification. We can investigate the effect of the layers by adding a layer to them. The two-layer in the geometry of shallow water is not only a layered liquid model, but also it is an excellent model of a wide range of ocean and atmospheric phenomena; see [23].

One way to depict fluid flow is as a multilayer flow, where one layer flows on top of another. This difference in a layer is caused by temperature differences, which lead to different densities. Ocean water can be viewed as a fluid with two layers. The temperature of the water in the first layer, which is sunlight-exposed water, is greater than the temperature of the second layer, which is below the first layer; see [23].

Shallow water flow in two layers, especially its exact and numerical solution, is an interesting subject to be studied. They particularly find the best-governing equation that can describe physical phenomena.

The two-layer fluid flow model over the inclined and flat bottom was investigated in [17]. The model utilized a non-Newtonian fluid. They used the flow of mud in the water to illustrate the model. Then, this model was solved analytically and numerically. The McCormack's scheme was used to obtain the numerical solution since this scheme is suitable for systems that meet the hyperbolic conservation law, and it has second-order accuracy. The numerical simulation of stratified fluid, supposed to be two-layer shallow water flows through a channel with irregular geometry, was studied in [5]. They proposed extensions of the Q-schemes of van Leer and Roe to get the numerical solution of the model. The central upwind was used to solve the two-layer shallow water equations [10].

Furthermore, the fluid flow model with inclined and uneven bottom was developed in [25]. In this model, it was assumed that the fluid had a single layer and flowed in horizontal and vertical directions. The constructed model was completed analytically and numerically using the finite difference method by applying periodic boundary conditions. A numerical scheme stability analysis was also performed using the Fourier analysis developed by Von

Neumann. The stability analysis revealed that the flow was stable, which means that the error of a numerical solution will not grow infinitely with time.

The analytical and numerical methods were developed quickly to find the best solution for the model. The analytical method is the best method to find the solution of the mathematical model since this method does not have any errors that appear from the truncation of the method itself. Unfortunately, analytical methods sometimes require some complex calculations and are very difficult to solve. To handle this problem, numerical methods can be used to approximate the solutions of the governing equations. The classical finite difference method, in which derivatives are approximated by finite difference, is a well-known method to approximate the solution. Discontinuities become a problem when they occur in the solution. Such a method can be used as well with certain treatments near discontinuities in the solution. The finite volume method (FVM) is a method based on an integral form instead of the differential equation. Rather than pointwise approximations at grid points, the FVM breaks the domain into grid cells and approximates the total integral over grid cells. This integral is divided by the volume of the cell. These values are changed at each step by the flux passing through the edges of the grid cells. The main problem is to determine the proper numerical flux function that properly approximates the correct flux [11].

The study of the two-layer shallow water system (flat bottom) analytically and numerically was investigated in [3]. For an analytical solution, they considered a relaxation approach, which offers greater decoupling and accessible eigenstructures. The numerical solution of a two-layer shallow water equation using the FVM with an explicit scheme was investigated in [7]. Then, Swartenbroekx, Zech, and Soares-Frazao [22] predicted the bed load transport induced by dam break waves by proposing two-dimensional (2D) two-layer shallow water equations, where the upper layer was made of clear water, and the lower layer was made of a dense mixture of water and moving grains. The governing equation of the model was solved by applying Harten–Lax–Van Lear Finite Volume Scheme and a well-balanced Roe method [9]. Recently, Muhammad [13] simulated the flowing fluid using the FVM via OpenFOAM.

On the other hand, the flat-bottomed shallow hydraulic analogy of the Gibraltar Strait was developed with wind stress in mind [6]. In this model, the flow was assumed to be quasi-horizontal. The y component was ignored ,and the density was uniform in each layer. The model was numerically solved using the FVM based on the Roe-Riemann scheme approach. Chiapolino and dan Saure [8] also derived a two-layer shallow water flow model with some limitations by ignoring the vertical velocity component and assuming that the velocity is uniform across the cross-sections of each layer. This model was solved numerically using the Godunov scheme, which is an approximation of the Riemann problem at each cell boundary. A method for the numerical solution of the nonlinear regularized long wave equation

was studied in [20]. They [19] proposed an implicit method for the time discretization based on the θ-weighted and finite difference methods, while the spatial discretization is described with the help of the finite difference scheme derived from the local radial basis function method (the local collocation method). The localized meshless collocation method was studied in [16, 15]. A new weighted essentially non-oscillatory (WENO), a finite difference Hermite RBF-WENO scheme, and a modified weighted essentially non-oscillatory (WENO) scheme are procedures for solving hyperbolic conservation laws were studied in [18, 1, 2].

The study conducted in [4] obtained a numerical solution of the advection-reaction-diffusion equation using the FVM. In the FVM, the integral form is used to discretize the equation. The discretization of space used the Quadratic Upwind Interpolation for Convective Kinematics (QUICK) scheme, while the discretization of time used an explicit, implicit, or Crank Nicolson scheme.

In this paper, we solve numerically a mathematical formula of a two-layer shallow water flow with slope and uneven bottom by using the FVM with a QUICK scheme to discretize the space domain and explicit scheme to discretize the time domain. The new one in this article is how to find a solution of the model when the bottom of the shallow water is not flat. The FVM is used to solve the model because this method is suitable for computational fluid dynamics problems. The QUICK method is chosen since it is a third-order scheme that provides good accuracy, and this scheme have been proven its numerical stability. The advantages of this method are that the main coefficients are positive and satisfy the requirements for conservativeness, boundedness, and transportiveness [24]. A numerical simulation of the solutions is presented to describe the behavior of this model.

The organization of this work is as follows: Section 2 derives the governing equations of the models in steady and unsteady states. In Section 3, the FVM is constructed as a numerical solution with the QUICK scheme for discretization. Section 4 provides numerical simulations of the shallow water flows with several given parameters. Finally, Section 5 ends up with a brief conclusion.

2 Governing equations

The governing equation of the two-layer shallow water with slope and the uneven bottom is described in Figure 1. It is a non-dimensional form after deriving from continuity and momentum equations of shallow water equations. For detailed calculating, revisit [12]. The equation reads as follows:

$$\frac{\partial}{\partial t}\left(\eta_1 - \eta_2\right) + \frac{\partial}{\partial x}\left(u_1(\eta_1 - \eta_2)\right) = 0, \tag{1}$$

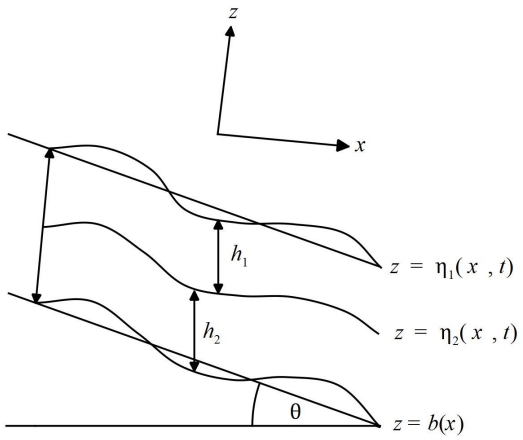

Figure 1: Two-layer shallow water flow with incline and uneven bottom [12].

$$\frac{\partial \eta_2}{\partial t} + \frac{\partial}{\partial x}\left(u_2(\eta_2 - b)\right) = 0, \tag{2}$$

$$\frac{\partial u_1}{\partial t} + u_1 \frac{\partial u_1}{\partial x} = -g\cos\theta \frac{\partial \eta_1}{\partial x} + g\sin\theta, \tag{3}$$

$$\frac{\partial u_2}{\partial t} + u_2 \frac{\partial u_2}{\partial x} = (g' - g)\cos\theta \frac{\partial \eta_1}{\partial x} - g'\cos\theta \frac{\partial \eta_2}{\partial x} + g\sin\theta. \tag{4}$$

We introduce the non-dimensional variables as follows:

$$x = L\widetilde{x}, \quad z = H\widetilde{z}, \quad t = \frac{L}{U}\widetilde{t}, \quad \eta_1 = H\widetilde{\eta}_1,$$
$$\eta_2 = H\widetilde{\eta}_2, \quad b = H\widetilde{b}, \quad q_1 = UH\widetilde{q}_1, \quad q_2 = UH\widetilde{q}_2,$$

and

$$U = (Hg')^{\frac{1}{2}}, \quad L = \frac{U^2}{g}, \quad \gamma = \frac{g'}{g},$$

where U is a typical velocity, L is typical length, and T is a typical time scale, and H is mean height. The two-layer shallow water with slope and uneven bottom in non-dimensional form is

$$\frac{\partial \eta_1}{\partial t} - \frac{\partial \eta_2}{\partial t} + \frac{\partial u_1\eta_1}{\partial x} - \frac{\partial u_1\eta_2}{\partial x} = 0, \tag{5}$$

$$\frac{\partial \eta_2}{\partial t} + \frac{\partial u_2\eta_2}{\partial x} - \frac{\partial u_2 b}{\partial x} = 0, \tag{6}$$

$$\frac{\partial u_1}{\partial t} + \frac{\partial}{\partial x}\left(\frac{u_1^2}{2}\right) = -\frac{\cos\theta}{\gamma}\frac{\partial \eta_1}{\partial x} + \sin\theta, \tag{7}$$

$$\frac{\partial u_2}{\partial t} + \frac{\partial}{\partial x}\left(\frac{u_2^2}{2}\right) = \left(1 - \frac{1}{\gamma}\right)\cos\theta\frac{\partial \eta_1}{\partial x} - \cos\theta\frac{\partial \eta_2}{\partial x} + \sin\theta. \tag{8}$$

We call the bottom layer as layer one, and the upper layer as layer two. We introduce the variables used in each layer, $p_1(x,t)$ and $p_2(x,t)$ are pressure forces in layers one and two. The upper layer has a pressure force $p_1(x,t)$, which is lower than the pressure force at the bottom layer $p_2(x,t)$. Then, $\eta_1(x,t)$ is the free-surface movement vertically while $\eta_2(x,t)$ is the distance between layers one and two's interface height, where $\eta_2(x,t) < z < \eta_1(x,t)$ and $b(x) < z < \eta_2(x,t)$. The thickness of the water columns is $h_1(x,t)$ and $h_2(x,t)$. The uneven bottom topography is $b(x)$, where, in general, $h_2(x,t) = \eta_2(x,t) - b(x)$, for the flat bottom $\eta_2(x,t) = h_2(x,t)$, and θ is the slope of the bottom surface. Moreover, $\gamma = g'/g$, where g is the gravitational force, and $g' = g(\frac{\rho_2 - \rho_1}{\rho_1})$ is the reduced gravity, while ρ_2 and ρ_1 are density in layers one and two. The proposed model, (1)–(4), is a powerful model of many geophysically interesting phenomena as well as being physically realizable in the laboratory [23].

2.1 Steady-state two-layer shallow water flow

In this part, shallow water is assumed to be in a steady state. This means at every point, the mass fluxes over the depth and energy are constant [14]. It is assumed that the height and water debit are constant with respect to time [21]. Equations (5)–(8) become

$$\frac{\partial u_1\eta_1}{\partial x} - \frac{\partial u_1\eta_2}{\partial x} = 0, \tag{9}$$

$$\frac{\partial u_2\eta_2}{\partial x} - \frac{\partial u_2 b}{\partial x} = 0, \tag{10}$$

$$0 = -\frac{\cos\theta}{\gamma}\frac{\partial \eta_1}{\partial x} + \sin\theta, \tag{11}$$

$$0 = \left(1 - \frac{1}{\gamma}\right)\cos\theta\frac{\partial \eta_1}{\partial x} - \cos\theta\frac{\partial \eta_2}{\partial x} + \sin\theta, \tag{12}$$

where $x \in [0, K]$ in which K is a constant at the boundary space domain. The equation system (9)–(12) is a function of spatial variable, such that the initial conditions for the equation system (9)–(12) are given as follows:

$$\eta_1(x,0) = \tan\theta x + A\sin(3x), \tag{13}$$

$$\eta_2(x,0) = \tan\theta x + A\sin(3x) - 3, \tag{14}$$

$$b(x) = \tan\theta x + K\tan\theta + A(\cos(5x) - \sin(3x)) - 4, \tag{15}$$

and the boundary conditions are given by

$$\eta_1(0) = \tan\theta(0) + A\sin(3(0)), \tag{16}$$
$$\eta_2(0) = \tan\theta(0) + A\sin(3(0)) - 3, \tag{17}$$
$$\eta_1(K) = \tan\theta(K) + A\sin(3(K)), \tag{18}$$
$$\eta_2(K) = \tan\theta(K) + A\sin(3(K)) - 3, \tag{19}$$
$$\frac{\partial\eta_1}{\partial x} = \frac{\partial\eta_2}{\partial x} = \tan\theta\gamma, \tag{20}$$

where A is wave amplitude.

The steady state of (9)–(12) can be applied to river at rest conditions. It seems that the river consists of two-layers. The temperature of the first layer will be lower than the temperature of the second layer when the river is exposed to sunshine. As a result, the first layer pressure is lower than the second layer pressure. The layers compete with one another when the interface between the two layers varies from position to position (wavy). Similarly, on an uneven base, generally, topography and bottom layer will exert forces on one another. Because it is in a steady state, the bottom shape is unevenly followed by the first and second levels. We will show this in numerical simulations.

2.2 Unsteady-state two-layer shallow water flow

For an unsteady state two-layer shallow water flow, it is assumed that the flow of shallow water at the upper free-surface, the gravitational force, is imposed on the fluid as the restoring force. Because we consider hydrostatic balance, the changes of surface velocity, and height are quite small around the depth of the h surface wave at constant conditions [23]. The depth of the fluid is as much as the displacement or movement of the free surface. We linearize (5)–(8) by defining new variables to describe the displacement of the fluid at rest; that is,

$$h_1(x,t) = H_1 + h_1'(x,t) = H_1 + (\eta_1'(x,t) - \eta_2'(x,t)), \tag{21}$$
$$h_2(x,t) = H_2 + h_2'(x,t) = H_2 + (\eta_2'(x,t) - b(x)), \tag{22}$$
$$u_1(x,t) = u_1'(x,t), \tag{23}$$
$$u_2(x,t) = u_2'(x,t). \tag{24}$$

Equations (21)–(24) are substituted into (5)–(8). Then, the variable following the derivation of steady state two-layer shallow water flow is non-dimensionalized. We obtain the following equations:

$$\frac{\partial\eta_1}{\partial t} - \frac{\partial\eta_2}{\partial t} = 0, \tag{25}$$
$$\frac{\partial\eta_2}{\partial t} + \frac{\partial u_2}{\partial x} - \frac{\partial u_2 b}{\partial x} = 0, \tag{26}$$

$$\frac{\partial u_1}{\partial t} = -\frac{\cos\theta}{\gamma}\frac{\partial \eta_1}{\partial x} + \sin\theta, \tag{27}$$

$$\frac{\partial u_2}{\partial t} = \left(1 - \frac{1}{\gamma}\right)\cos\theta\frac{\partial \eta_1}{\partial x} - \cos\theta\frac{\partial \eta_2}{\partial x} + \sin\theta, \tag{28}$$

where $x \in [0, K], t \in [0, L]$, with the initial conditions of the flow is stationary and the speed of the water remains along the channel

$$\eta_1(x, 0) = \tan\theta x + A\sin(3x), \tag{29}$$

$$\eta_2(x, 0) = \tan\theta x + A\sin(3x) - 3, \tag{30}$$

$$b(x) = \tan\theta x + K\tan\theta + A(\cos(5x) - \sin(3x)) - 4, \tag{31}$$

$$u_1(x, 0) = u_2(x, 0) = 0, \tag{32}$$

and the boundary condition is assumed that the flow is not moving, so that the velocity is equal to zero. The boundary condition of unsteady state two-layer shallow water flow is periodic functions as follows:

$$\eta_1(0, t) = \tan\theta(0) + A\sin(3(0)), \tag{33}$$

$$\eta_2(0, t) = \tan\theta(0) + A\sin(3(0)) - 3, \tag{34}$$

$$\eta_1(K, t) = \tan\theta(K) + A\sin(3(K)), \tag{35}$$

$$\eta_2(K, t) = \tan\theta(K) + A\sin(3(K)) - 3, \tag{36}$$

$$\frac{\partial \eta_1(0, t)}{\partial x} = \frac{\partial \eta_2(0, t)}{\partial x} = \tan\theta\gamma + 3A\cos(3(0)), \tag{37}$$

$$u_1(0, t) = u_2(0, t) = 0, \tag{38}$$

where $x > 0$ and $t > 0$.

3 Finite volume method (FVM)

The FVM is a technique using integral form rather than differential equations. Pointwise estimates at grid points are preferred. The domain is divided into grid cells by the FVM, which then approximates the entire integral over the grid cells. This integral is divided by the volume of the cells. The value changes at each step depending on the flow passing through the edges of the grid cells. The main problem is determining the appropriate numerical flow function that is directly close to the true flow [11].

By following the procedure in [24], we integrate the governing equations for steady and unsteady state, (9)–(12) and (25)–(28), respectively, along control volume and time. Furthermore, we use QUICK scheme to discretize space domain and explicit scheme to discretize time domain.

Here, we summarize the procedure of the proposed method as follows:

1. **Grid generation**
   The first step in the FVM is to divide the domain into discrete control volumes. Let us place a number of nodal points in the space between A and B. The boundaries (or faces) of control volumes are positioned mid-way between adjacent nodes. Thus each node is surrounded by a control volume or cell. It is common practice to set up control volumes near the edge of the domain in such a way that the physical boundaries coincide with the control volume boundaries.

2. **Discretisation**
   The key step of the FVM is the integration of the governing equation (or equations) over a control volume to yield a discretized equation at its nodal point P.

3. **Solution of equations**
   The resulting system of linear algebraic equations is then solved to obtain the distribution of the solution at nodal points.

3.1 Steady-state FVM

To solve (9)–(12) by using the FVM, first, we integrate (10) with respect to Control Volume (CV) as follows:

$$\int_{CV} \left(\frac{\partial u_2 \eta_2}{\partial x} - \frac{\partial u_2 b}{\partial x} \right) dV = 0. \tag{39}$$

This is the equation related to the first layer of shallow water flow. Since the model of two-layer shallow water flow has one dimension in space, the CV can be described as in [24]. Then (39) becomes

$$A\left(u_{2e} - u_{2w}\right)\left(\eta_{2e} - \eta_{2w}\right) = A\left(u_{2e} - u_{2w}\right)\left(b_e - b_w\right), \tag{40}$$

where index e is the east face and w is the west face. By applying QUICK discretization, we transform the control face to be nodal and after simplifying (40). Then we get

$$\frac{1}{8}\eta_{2WW} - \frac{7}{8}\eta_{2W} + \frac{3}{8}\eta_{2P} + \frac{3}{8}\eta_{2E} = \frac{1}{8}b_{WW} - \frac{7}{8}b_W + \frac{3}{8}b_P + \frac{3}{8}b_E. \tag{41}$$

Equation (41) can be written as a linear equation of the system by substituting $i = 2, 3, \ldots, N-1$ and applying initial and boundary condition such that we have

$$\begin{bmatrix} \frac{3}{8} & \frac{3}{8} & 0 & 0 & \cdots & 0 & 0 & 0 & 0 \\ \frac{-7}{8} & \frac{3}{8} & \frac{3}{8} & 0 & \cdots & 0 & 0 & 0 & 0 \\ \frac{1}{8} & \frac{-7}{8} & \frac{3}{8} & \frac{3}{8} & \cdots & 0 & 0 & 0 & 0 \\ \vdots & \vdots & \vdots & \vdots & \ddots & 0 & 0 & 0 & 0 \\ 0 & 0 & 0 & 0 & \cdots & \frac{1}{8} & \frac{-7}{8} & \frac{3}{8} & \frac{3}{8} \\ 0 & 0 & 0 & 0 & \cdots & 0 & \frac{1}{8} & \frac{-7}{8} & \frac{3}{8} \end{bmatrix} \begin{bmatrix} \eta_{2\,2} \\ \eta_{2\,3} \\ \eta_{2\,4} \\ \vdots \\ \eta_{2\,K-2} \\ \eta_{2\,K-1} \end{bmatrix} = \begin{bmatrix} F_2 \\ F_3 \\ F_4 \\ \vdots \\ F_{K-2} \\ F_{K-1} \end{bmatrix}, \tag{42}$$

with

$$\begin{bmatrix} F_2 \\ F_3 \\ F_4 \\ \vdots \\ F_{K-2} \\ F_{K-1} \end{bmatrix} = \begin{bmatrix} -\frac{6}{8}b_{i-1} + \frac{1}{8}\Delta x T1 + \frac{3}{8}b_i + \frac{3}{8}b_{i+1} + \frac{6}{8}\eta_{2\,i-1} - \frac{1}{8}\Delta x \tan(\theta)\gamma \\ \frac{1}{8}b_{i-2} - \frac{7}{8}b_{i-1} + \frac{3}{8}b_i + \frac{3}{8}b_{i+1} - \frac{1}{8}\eta_{2\,i-2} \\ \frac{1}{8}b_{i-2} - \frac{7}{8}b_{i-1} + \frac{3}{8}b_i + \frac{3}{8}b_{i+1} \\ \vdots \\ \frac{1}{8}b_{i-2} - \frac{7}{8}b_{i-1} + \frac{3}{8}b_i + \frac{3}{8}b_{i+1} \\ \frac{1}{8}b_{i-2} - \frac{7}{8}b_{i-1} + \frac{3}{8}b_i + \frac{3}{8}b_{i+1} - \frac{3}{8}\eta_{2\,i+1} \end{bmatrix},$$

where $T_1 = \tan\theta + A(5\sin(-5(0)) - 3\cos(-3x(0)))$. The methods for solving a system of linear equations can be used to determine the value of η_{2i}, for example, Thomas's algorithm.

Furthermore, similar to the first layer, the discretization equation of the second layer is obtained by integrating (9) with respect to CV

$$\int_{CV} \left(\frac{\partial u_1 \eta_1}{\partial x} - \frac{\partial u_1 \eta_2}{\partial x} \right) dV = 0. \tag{43}$$

Discretization QUICK is applied to (43) by following the procedure in [24] and applying initial and boundary conditions. Then, we arrive at a system of linear equations as follows:

$$\begin{bmatrix} \frac{3}{8} & \frac{3}{8} & 0 & 0 & \cdots & 0 & 0 & 0 & 0 \\ \frac{-7}{8} & \frac{3}{8} & \frac{3}{8} & 0 & \cdots & 0 & 0 & 0 & 0 \\ \frac{1}{8} & \frac{-7}{8} & \frac{3}{8} & \frac{3}{8} & \cdots & 0 & 0 & 0 & 0 \\ \vdots & \vdots & \vdots & \vdots & \ddots & 0 & 0 & 0 & 0 \\ 0 & 0 & 0 & 0 & \cdots & \frac{1}{8} & \frac{-7}{8} & \frac{3}{8} & \frac{3}{8} \\ 0 & 0 & 0 & 0 & \cdots & 0 & \frac{1}{8} & \frac{-7}{8} & \frac{3}{8} \end{bmatrix} \begin{bmatrix} \eta_{1\,2} \\ \eta_{1\,3} \\ \eta_{1\,4} \\ \vdots \\ \eta_{1\,K-2} \\ \eta_{1\,K-1} \end{bmatrix} = \begin{bmatrix} G_2 \\ G_3 \\ G_4 \\ \vdots \\ G_{K-2} \\ G_{K-1} \end{bmatrix}, \tag{44}$$

with

$$\begin{bmatrix} G_2 \\ G_3 \\ G_4 \\ \vdots \\ G_{K-2} \\ G_{K-1} \end{bmatrix} = \begin{bmatrix} -\frac{6}{8}\eta_{2i-1} + \frac{1}{8}\Delta x\tan(\theta)\gamma + \frac{3}{8}\eta_{2i} + \frac{3}{8}\eta_{2i+1} + \frac{6}{8}\eta_{2i-1} - \frac{1}{8}\Delta x\tan(\theta)\gamma \\ \frac{1}{8}\eta_{2i-2} - \frac{7}{8}\eta_{2i-1} + \frac{3}{8}\eta_{2i} + \frac{3}{8}\eta_{2i+1} - \frac{1}{8}\eta_{1i-2} \\ \frac{1}{8}\eta_{2i-2} - \frac{7}{8}\eta_{2i-1} + \frac{3}{8}\eta_{2i} + \frac{3}{8}\eta_{2i+1} \\ \vdots \\ \frac{1}{8}\eta_{2i-2} - \frac{7}{8}\eta_{2i-1} + \frac{3}{8}\eta_{2i} + \frac{3}{8}\eta_{2i+1} \\ \frac{1}{8}\eta_{2i-2} - \frac{7}{8}\eta_{2i-1} + \frac{3}{8}\eta_{2i} + \frac{3}{8}\eta_{2i+1} - \frac{3}{8}\eta_{1i+1} \end{bmatrix}.$$

The value of η_{1i} can be obtained by the methods for solving system of linear equations.

3.2 Unsteady-state FVM

For unsteady-state two-layer shallow water flow, we integrated (25)–(28) with respect to CV and time. The procedure to get the integration (25)–(28) with respect to CV in the unsteady state, shallow water flow is similar to the procedure to calculate the integral of the governing equation in the steady state. We apply QUICK discretization. The difference is we integrate the governing equation with respect to time, and apply an explicit scheme for discretization. First, we integrate (25) to yield

$$\int_t^{t+\Delta t}\int_{CV}\left(\frac{\partial\eta_1}{\partial t} - \frac{\partial\eta_2}{\partial t}\right)dV\,dt = 0. \tag{45}$$

The result of the integration of (45) is

$$(\eta_{1P} - {\eta_1}_P^0)A\Delta x - (\eta_{2P} - {\eta_2}_P^0)A\Delta x = 0, \tag{46}$$

where $\eta_{1,P}$ and $\eta_{2,P}$ are the height of surface at node P and time $t+\Delta t$, $\eta_{1,P}^0$ and $\eta_{2,p}^0$ are the height of surface at node P and time t. By simplifying (46) and writing the index P becomes i, we get the height of the first layer

$${\eta_1}_i^{n+1} = {\eta_1}_i^n + {\eta_2}_i^{n+1} - {\eta_2}_i^n, \tag{47}$$

where the subscribe n denotes time t, and $n+1$ denotes time $t+\Delta t$. We apply the procedure in [24] for the rest of (26)–(28), so that we obtain

$${\eta_2}_i^{n+1} = {\eta_2}_i^n - \frac{\Delta t}{\Delta x}\left(\frac{1}{8}{u_2}_{i-2}^n - \frac{7}{8}{u_2}_{i-1}^n + \frac{3}{8}{u_2}_i^n + \frac{3}{8}{u_2}_{i+1}^n\right)\left(1 - \left(\frac{1}{8}b_{i-2} - \frac{7}{8}b_{i-1} + \frac{3}{8}b_i + \frac{3}{8}b_{i+1}\right)\right). \tag{48}$$

$$u_1{}_i^{n+1} = u_1{}_i^{n} - \frac{\Delta t}{\Delta x}\frac{\cos\theta}{\gamma}\left(\frac{1}{8}\eta_1{}_{i-2}^{n} - \frac{7}{8}\eta_1{}_{i-1}^{n} + \frac{3}{8}\eta_1{}_{i}^{n} + \frac{3}{8}\eta_1{}_{i+1}^{n}\right) + \sin\theta\Delta t. \tag{49}$$

$$u_2{}_i^{n+1} = u_2{}_i^{n} + \frac{\Delta t}{\Delta x}\left(1 - \frac{1}{\gamma}\right)\cos\theta\left(\frac{1}{8}\eta_1{}_{i-2}^{n} - \frac{7}{8}\eta_1{}_{i-1}^{n}\frac{3}{8}\eta_1{}_{i}^{n} + \frac{3}{8}\eta_1{}_{i+1}^{n}\right) - \frac{\Delta t}{\Delta x}\cos\theta\left(\frac{1}{8}\eta_2{}_{i-2}^{n} - \frac{7}{8}\eta_2{}_{i-1}^{n} + \frac{3}{8}\eta_2{}_{i}^{n} + \frac{3}{8}\eta_2{}_{i+1}^{n}\right) + \sin\theta\Delta t. \tag{50}$$

The explicit solver is easily programmed, yet the time step t must be limited to stabilize the scheme. Experience has shown that we can simply enforce the Von Neumann criteria for the single step algorithm,

$$\left|\frac{\Delta t}{\Delta x}\right| < \frac{1}{2}. \tag{51}$$

4 Numerical simulation

Numerical simulation aims to illustrate movement of shallow water flows based on the numerical scheme obtained in the previous section. Numerical simulations are performed under the environment of MATLAB R2018a based on MacOS MOJAVE version 10.14.6, which the processor is 1.6 GHz Intel Core i5. Numerical solutions of steady-state of two-layer shallow water flow are calculated at $x \in [0, 5]$ by taking $\Delta x = 0.1$ and $\gamma = 1$ [17]. Figure 2 depicts two shallow water layers at rest, where the water velocity is zero and there is no time-dependent flow movement. Changes at the bottom surface are followed by depth changes at the first and second chamber levels. When we increase the slope, the depth of the second layer is higher than the first layer. The two-layer shallow water flow conditions remain stable for each slope of (θ). Negative sign of slope has physical interpretation, that is, water flows from the left side to the right side. Figure 3 shows the velocity profiles of steady-state of two-layer shallow water flow at $t = 0.025$.

Table 1: Comparison of the CPU run times of the proposed method depends on the slopes.

$\theta = -10$	$\theta = -30$	$\theta = -60$
1,376413 second	1,536349 second	1,544937 second

Furthermore, the numerical simulation for unsteady-state two-layer shallow water flow can be seen in Figures 4 and 5. The parameter (γ), slope (θ), and space domain for the simulation are chosen with the same values for the steady-state. The time domain is $t \in [0, 0.1]$ with $\Delta t = 0.001$. The simulated water wave height and velocity are calculated when $t = 0.025$ and $t = 0.1$. The height profile of unsteady-state two-layer shallow water flow at $t = 0.025$

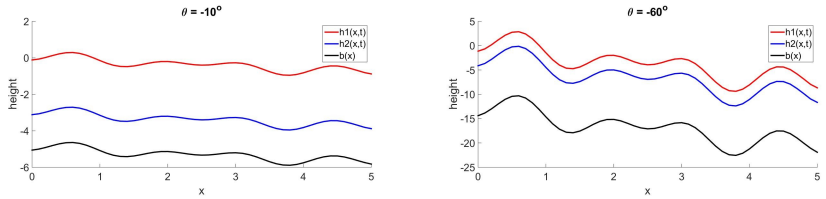

Figure 2: The numerical solution of steady-state of two-layer shallow water flow with $\theta = 10^0$, $\theta = 30^0$, and $\theta = 60^0$.

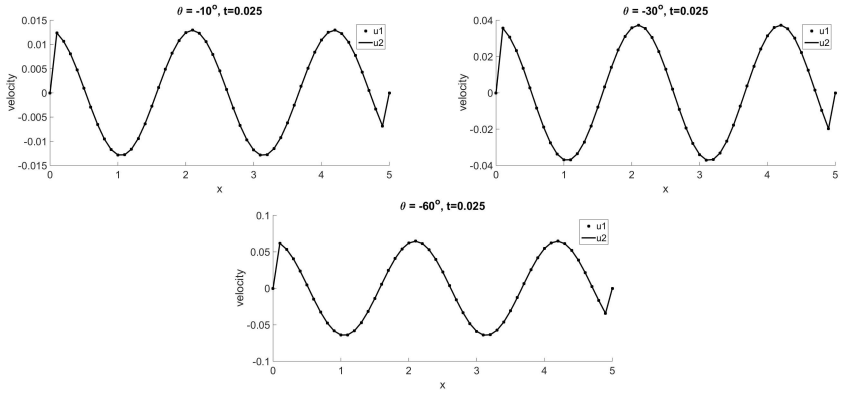

Figure 3: The velocity profiles of steady-state of two-layer shallow water flow at $t = 0.025$.

is shown in Figure 4, while the velocity profiles of unsteady-state of two-layer shallow water flow at $t = 0.025$ is shown in Figure 5.

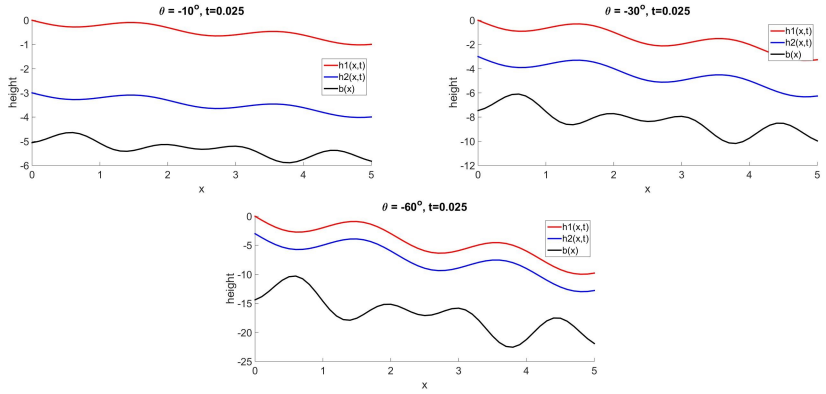

Figure 4: The height profiles of unsteady-state two-layer shallow water flow at $t = 0.025$.

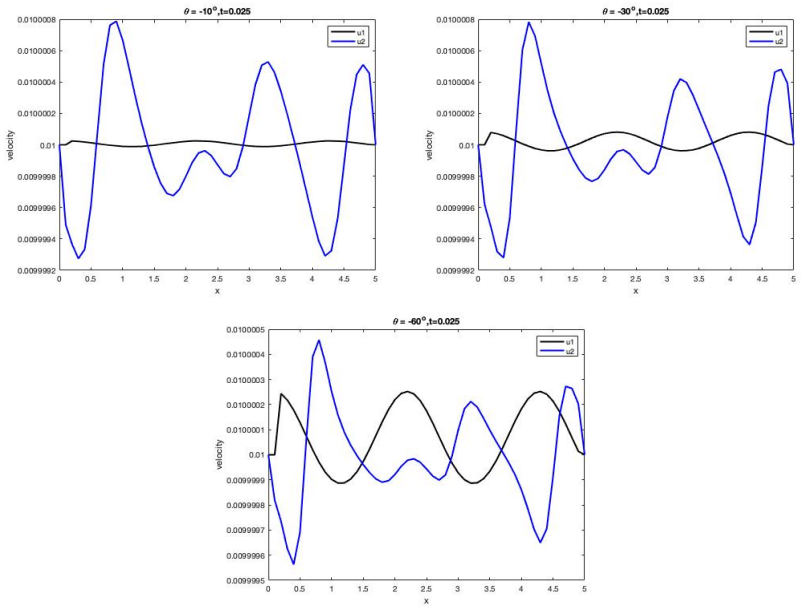

Figure 5: The velocity profiles of unsteady-state of two-layer shallow water flow at $t = 0.025$.

The numerical solution for unsteady shallow water produces instability (see Figure 5). It is because there is a compressive force between the layers. Similarly, if the liquid's bottom is not flat, the bottom layer and topography tend to push against one another. This type of force, known as form drag. Moreover, in Figure 5, when the slope is increased, the depth of the second layer is higher than the first layer, and the second layer has a more wavy shape than the first layer. In Figure 5, the flow has bigger velocity when the slope of bottom layer is increased. From Table 2, the velocity at layer one increases when the slope is increased. Similarly, the velocity at layer two increases when the slope is increased see Table 3. The last row in each Tables 2 and 3 shows the rate of velocity u_1 and u_2. The CPU run times of the proposed method is written in Table 1.

Table 2: Comparison of velocity u_1 depends on the slopes.

u_1 at $\theta = -10$	u_1 at $\theta = -30$	u_1 at $\theta = -60$
0,01	0,01	0,01
0,01	0,01	0,01
0,010000047	0,010000156	0,010000486
0,010000042	0,01000014	0,010000435
0,010000035	0,010000115	0,010000356
0,010000025	0,010000084	0,010000257
0,010000015	0,010000049	0,010000148
0,010000004	0,010000013	0,01000004
0,009999994	0,00999998	0,009999941
0,009999986	0,009999953	0,009999861
0,00999998	0,009999934	0,009999804
0,009999976	0,009999924	0,009999775
0,009999977	0,009999924	0,009999776
0,00999998	0,009999934	0,009999806
0,009999986	0,009999954	0,009999864
0,009999995	0,009999982	0,009999946
0,010000005	0,010000015	0,010000046
0,010000015	0,010000051	0,010000154
0,010000026	0,010000086	0,010000263
0,010000035	0,010000117	0,010000361
0,010000043	0,010000141	0,010000439
0,010000047	0,010000157	0,010000489
0,010000049	0,010000162	0,010000504
0,010000047	0,010000156	0,010000485
0,010000042	0,010000139	0,010000431
0,010000034	0,010000114	0,010000351
0,010000025	0,010000082	0,010000251
0,010000014	0,010000047	0,010000142
0,010000003	0,010000011	0,010000034
0,009999993	0,009999979	0,009999936
0,009999985	0,009999952	0,009999857
0,009999979	0,009999933	0,009999801
0,009999976	0,009999923	0,009999774
0,009999977	0,009999924	0,009999776
0,00999998	0,009999935	0,009999809
0,009999986	0,009999956	0,009999868
0,009999995	0,009999984	0,009999951
0,010000005	0,010000017	0,010000051
0,010000016	0,010000053	0,01000016
0,010000027	0,010000088	0,010000268
0,010000036	0,010000118	0,010000366
0,010000043	0,010000142	0,010000442
0,010000047	0,010000157	0,01000049
0,010000049	0,010000162	0,010000504
0,010000047	0,010000155	0,010000483
0,010000042	0,010000138	0,010000428
0,010000034	0,010000112	0,010000346
0,010000024	0,01000008	0,010000245
0,010000013	0,010000045	0,010000136
0,010000003	0,010000009	0,010000028
0,01	0,01	0,01
0,510000685	0,51000228	0,510007164

Table 3: Comparison of velocity u_2 depends on the slopes.

u_2 at $\theta = -10$	u_2 at $\theta = -30$	u_2 at $\theta = -60$
0,01	0,01	0,01
0,009999236	0,009999431	0,009999728
0,009999233	0,009999349	0,009999664
0,009999146	0,00999918	0,009999542
0,009999225	0,009999147	0,009999474
0,009999545	0,009999439	0,009999622
0,010000052	0,010000062	0,01000004
0,010000542	0,01000064	0,010000417
0,010000821	0,010000851	0,010000502
0,010000857	0,010000764	0,010000407
0,010000736	0,010000576	0,010000283
0,01000055	0,01000039	0,010000182
0,010000354	0,010000236	0,010000106
0,010000169	0,010000109	0,010000049
0,01	0,010000001	0,010000001
0,009999849	0,009999904	0,009999958
0,009999721	0,009999815	0,009999917
0,009999628	0,00999974	0,00999988
0,009999584	0,009999691	0,009999852
0,009999598	0,009999681	0,009999842
0,009999659	0,009999714	0,009999853
0,009999739	0,00999977	0,009999879
0,009999804	0,009999822	0,009999904
0,009999833	0,009999847	0,009999917
0,009999824	0,009999841	0,009999915
0,009999795	0,009999816	0,009999902
0,00999977	0,009999793	0,009999889
0,009999785	0,009999802	0,009999893
0,00999987	0,00999988	0,009999935
0,01000004	0,010000044	0,010000027
0,010000262	0,010000256	0,010000145
0,010000465	0,010000426	0,01000023
0,01000058	0,010000443	0,010000214
0,010000494	0,010000344	0,010000159
0,010000353	0,010000229	0,010000102
0,010000189	0,010000116	0,01000005
0,010000014	0,010000006	0,010000002
0,009999831	0,009999893	0,009999953
0,009999641	0,009999768	0,009999897
0,009999446	0,00999962	0,009999826
0,009999266	0,00999945	0,009999736
0,009999147	0,009999283	0,009999632
0,009999163	0,009999199	0,009999553
0,009999371	0,009999324	0,009999592
0,009999739	0,009999699	0,009999808
0,010000128	0,010000137	0,010000082
0,010000397	0,010000409	0,010000239
0,0100005	0,010000471	0,010000259
0,010000565	0,010000492	0,010000257
0,01	0,01	0,01
0,509997101	0,509997386	0,509998561

5 Conclusion

In this research, we offered a numerical solution for a two-layer shallow water flow with slope and uneven bottom for both steady-state and unsteady-state. The QUICK and explicit schemes were used to determine the numerical solution through the FVM. The steady-state numerical solution yielded stable results, while unsteady-state numerical solutions produced unstable results. The momentum that can be added to or taken from a flow, is what leads to this instability. This happened when there are differences in the position or surface wave shape between the first and second layers. The layers exert a compressive force on one another. Similar to this, if the fluid's bottom is not flat, the bottom layer and the topography will generally exert forces on one another. Moreover, the simulations yielded the larger slope resulted in higher velocity and higher depth at second layer.

Acknowledgments

The authors would like to express their gratitude to Prof. Sukir Maryanto for valuable comments of the research, and LPPM of Brawijaya University.

References

[1] Abedian, R. *A modified high-order symmetrical WENO scheme for hyperbolic conservation laws*, Int. J. Nonlinear Sci. Numer. Simul. 2022.

[2] Abedian, R. *A finite difference Hermite RBF-WENO scheme for hyperbolic conservation laws*, Int. J. Numer. Methods Fluids, 94(6) (2022), 583–607.

[3] Abgrall, R. and Karni, S. *Two-layer shallow water system: A relaxation approach*, SIAM J. Sci. Comput. 31(3) (2009), 1603–1627.

[4] Arachchige, J.P. and Pettet. G.J. *A finite volume method with linearisation in time for the solution of advection–reaction–diffusion systems*, Appl. Math. Comput. 231 (2014), 445–462.

[5] Castro, M.J., Garcia-Rodriguez, J.A., Gonzalez-Vida, J.M., Macias, J., Pares, C. and Vazquez-Cendon, M.E. *Numerical simulation of two-layer shallow water flows through channels with irregular geometry*, J. Comput. Phys. 195 (2004), 2002–235.

[6] Chakir, M., Ouazar, D., and Taik, A. *Roe scheme for two-layer shallow water equations: Application to the strait of Gibraltar*, Math. Model. Nat. Phenom. 4(5) (2009), 114–127.

[7] Chen, S C., and Peng, S.H. *Two-dimensional numerical model of two-layer shallow water equations for confluence simulation*, Adv. Water Resour. 29 (2006), 1608–1617.

[8] Chiapolino, A. and dan Saurel, R. *Models and methods for two-layer shallow water flows*, J. Comput. Phys. 371 (2018), 1043–1066.

[9] Cristo, C.D., Greco, M., Iervolino, M., Martino, R. and Vacca, A. *A remark of finite volume methods for 2D shallow water equations over irregular bottom topography*, J. Hydraul. Res. 59 (2021), 337–344.

[10] Kurganov, A. and Petrova, G. *Central-upwind schemes for two-layer shallow water equations*, SIAM J. Sci. Comput. 31(3) (2009), 1742–1773.

[11] Leveque, R.A. *Finite-volume methods for hyperbolic problems*. Cambridge University Press, 2002.

[12] Lina, I.R., Habibah, U., and Kusumawinahyu, W.M. *Mathematical modelling of two layer shallow water flow with incline and uneven bottom*, J. Phys. Conf. Ser. 1563 (2020), 0122019.

[13] Muhammad, N. *Finite volume method for simulation of flowing fluid via OpenFOAM*, Eur. Phys. J. Plus, 136 (10) (2021) 1–22.

[14] Mungkasi, S. *Finite volume methods for one-dimensional shallow water equations*. Ph.D. Thesis, Australian National University, 2008.

[15] Nikan, O. and Avazzadeh, Z.*Coupling of the Crank–Nicolson scheme and localized meshless technique for viscoelastic wave model in fluid flow*, J. Comput. Appl. Math. 398 (2021), 113695.

[16] Nikan, O., Avazzadeh, Z. and Rasoulizadeh, M.N. *Soliton solutions of the nonlinear sine-Gordon model with Neumann boundary conditions arising in crystal dislocation theory*, Nonlinear Dyn. 106 (2021), 783–813.

[17] Pascal, J.P. *A model for two-layer moderate Reynolds number flow down an incline*, Int. J. Non-Linear Mech. 36(6) (2001), 977–985.

[18] Rasoulizadeh, M.N., Ebadi, M.J., Avazzadeh, Z., and Nikan, O. *A high-order symmetrical weighted hybrid ENO-ux limiter scheme for hyperbolic conservation laws*, Comput. Phys. Commun. 185 (2014), 106–127.

[19] Rasoulizadeh, M.N., Ebadi, M.J., Avazzadeh, Z. and Nikan, O. *An efficient local meshless method for the equal width equation in fluid mechanics*, Eng. Anal. Bound Elem. 131 (2021), 258–268.

[20] Rasoulizadeh, M.N., Nikan, O. and Avazzadeh, Z. *The impact of LRBF-FD on the solutions of the nonlinear regularized long wave equation*, Math. Sci. 15 (2021), 365–376.

[21] Remi, A. and Smadar, K. *Two-layer shallow water system: A relaxation approach*, SIAM J. Sci. Comput. 31(3) (2009), 1603–1627.

[22] Swartenbroekx, C., Zech, Y.V. and Soares-Frazao, S. *Two-dimensional two-layer shallow water model for dam break flows with significant bed load transport*, Int. J. Numeric. Met, Fluids, 73 (2013), 477–508.

[23] Vallis, G.K. *Atmospheric and oceanic fluid dynamics*. Cambridge University Press, USA, 2006.

[24] Versteeg, H. K. and Malalasekera, W. *An introduction to computational fluid dynamics: The finite volume method*, Pearson Education Limited, 2007.

[25] Yadav, A., Chakraborty, S. and Usha, R. *Steady solution of an inverse problem in gravity-driven shear-thinning film flow: Reconstruction of an uneven bottom substrate*, J. Non-Newton. Fluid Mech. 219 (2015), 65–77.

How to cite this article
Habibah, U., Lina, I.R. and Kusumawinahyu, W.M., Two-layer shallow water formula with slope and uneven bottom solved by finite volume method. *Iran. j. numer. anal. optim.*, 2023; 13(2): 317-335. https://doi.org/10.22067/ijnao.2022.79205.1190